CrystEngComm

Cite this: *CrystEngComm*, 2011, **13**, 4689

www.rsc.org/crystengcomm

PAPER

Morphology evolution route of PbS crystals *via* environment-friendly electrochemical deposition†

Weiming Qiu,[a] Mingsheng Xu,[a] Fei Chen,[b] Xi Yang,[a] Yaxiong Nan[a] and Hongzheng Chen*[a]

Received 20th February 2011, Accepted 13th April 2011
DOI: 10.1039/c1ce05225j

We report the detailed roadmap of the morphology evolution of semiconductor PbS crystals synthesized by a green route. Without using any surfactant in our electrochemical deposition process, we obtained rich morphologies of PbS crystals in a bulk amount with uniform size, showing continuous shape change from octahedral to star-like, then to football-like, and finally to cubic morphology, by simple control over the $PbCl_2$ precursor concentration. We discuss such a morphology evolution in detail on the basis of the relative contributions of branching growth and capping effects of the Cl^- ions.

Introduction

The synthesis of semiconductor crystals with well-defined shapes, sizes, and structures has attracted extraordinary interest in order to realize their unique properties that not only depend on their chemical composition, but also on their shape, structure, phase, size, and size distribution.[1–3] So far, it is still a major challenge to develop facile, cost-effective, and environment-friendly routes without using auxiliary solvents and/or surfactants for the shape-controlled synthesis of semiconductor crystals.[4,5] Among various synthesis methods, electrochemical deposition represents a low-cost, flexible, and scalable method, which takes the advantages of rapid synthesis, low temperature, and a high degree of freedom in manipulating and monitoring the crystal growth directly on a substrate by varying deposition potential, deposition time, temperature, precursors, and precursor concentrations.[6] Moreover, it also enables the selected-area fabrication of micro/nanostructures by patterning the conductive areas.[7] Using this method, diverse semiconductor micro/nanostructures, such as ZnO nanorod and nanotube arrays,[8–10] Cu_2O microcrystals with various morphologies,[11–13] CuTe nanoribbons,[14] Bi_2Te_3 hierarchical nanostructures,[15] and conifer-like CdS films,[16] have been obtained recently.

Lead sulfide (PbS), an important direct band gap semiconductor with a narrow bandgap (0.41 eV) and a large exciton Bohr radius (18 nm),[17] has been intensively studied due to its potential applications such as for novel thermoelectric cells, photovoltaic cells, mid- and near-infrared emission and detection, and photodegradation of dyes.[18–22] Extensive effort has been devoted to develop effective approaches for the synthesis of PbS crystals with tunable sizes and shapes. For example, sphere-, cubic- and rod-shaped PbS nanocrystals were obtained by hot-injection method, where hazardous trioctylphosphine (TOP) or tributylphosphine (TBP), toxic trioctylphosphine oxide (TOPO) or oleylamine (OA) and other long chain amines were used as solvents and capping agents.[22–24] Hyperbranched PbS nanowires and nanowire pine trees were prepared by using a complicated chemical vapor deposition system.[25,26] By using TBP in toluene as a cation exchange promoter, PbS nanorods were synthesized by converting CdS nanorods through a Cu_2S intermediate.[27,28] Monodisperse PbS nanoflowers were prepared by a facile approach attributed to the coexistence of two types of amines with different-length alkyl chains and different steric hinderance.[29] With capping/stabilizing functions of surfactants such as toxic cetyltrimethylammonium bromide (CTAB) or biomolecules such as L-cysteine at high temperature (>150 °C), PbS crystals with a variety of different morphologies were synthesized by hydro- and polymer-assisted solvothermal methods.[4,29–33] However, most of the above methods involved either hazardous solvents and/or toxic surfactants (capping agents) that are not easily removed and may play an undesirable role in PbS applications, leading to non-green or complex processes. Although there were reports on the preparation of PbS films by electrochemical deposition (electrodeposition) method,[34,35] there are few reports on the controlled synthesis of PbS crystals by this method. Recently, we performed a preliminary synthesis of octahedral PbS microcrystals by electrodeposition, which were used as seeds for the subsequent hydrothermal growth of maya-pyramid PbS crystals.[36] On the other hand, despite several reports of shape evolution of crystals,[37–39] there are few observations on a continuous morphological change. Here, we report on a complete route of the shape evolution of PbS crystals on indium tin oxide (ITO) substrate by exploiting an electrodeposition

[a]*State Key Lab of Silicon Materials, MOE Key Laboratory of Macromolecule Synthesis and Functionalization, & Department of Polymer Science and Engineering, Zhejiang University, Hangzhou 310027, P. R. China. E-mail: hzchen@zju.edu.cn*
[b]*Laboratory of Polymer Materials and Engineering, Ningbo Institute of Technology, Zhejiang University, Ningbo 315100, P. R. China*
† Electronic supplementary information (ESI) available. See DOI: 10.1039/c1ce05225j

method without using any surfactant at 110 °C, demonstrating a green approach to freely achieve PbS crystals with uniform sizes. We show the successive evolution of PbS crystals from octahedral shapes, to star-like, to football-like, and finally to cubic shape and address the involved growth mechanism by elucidating the effect of the $PbCl_2$ precursor, in particular the concentration of Cl^- ions, deposition time, and the applied deposition current.

Experimental

Fabrication of PbS crystals by electrodeposition method

All chemicals used in this work were commercially available and used directly without further treatment. The electrochemical deposition experiments were carried out on an electrochemical workstation (CHI Instrument 660A) using galvanostatic mode, where the etched indium-tin oxide (ITO) glass (20 Ω/square) was used as a working electrode and the Pt plate as the counter electrode. Both electrodes were immersed vertically into the electrolyte solution containing $PbCl_2$ and sublimed sulfur (S) as precursors and a DMSO-H_2O mixture as the component solvent that was preheated to a setting temperature. The ITO substrates were rinsed ultrasonically in acetone, ethanol, and distilled water successively before use. In a typical process, a preselected amount of $PbCl_2$ and S powder was added into 90 mL of DMSO. After the completely dissolution of $PbCl_2$ and S powder, 20 mL of deionized water was added and then the mixture was kept at 110 °C, thereafter the electrochemical deposition experiment was typically proceeded for a preselected deposition time (75 s) at a constant current (0.2 mA). Note that the deposition area on the cathode as well as the overall volume of the DMSO-H_2O mixture were the same for all of our experiments. So, for simplicity, we used the deposition current and precursor amount to represent the deposition current density and the precursor concentration in this paper. The resulting PbS crystals deposited on ITO glass were rinsed with hot DMSO solvent and dried at 80 °C.

Characterization

The as-prepared PbS crystals were characterized by X-ray diffraction (XRD) patterns on a Rigaku D/max-2550PC X-ray diffractometer with Cu-Kα radiation (λ = 1.5406 Å). EBSD analysis of the crystallographic orientation of the PbS crystals on ITO substrate was carried out using a JSM–7001F field-emission scanning electron microscopy (SEM) system with an accelerating voltage of 20 kV. SEM images taken on an S-4800 or JSM-7001 F scanning electron microscope were used to determine the shape evolution of the PbS crystals deposited on the ITO glass.

Results and discussion

X-Ray diffraction (XRD) measurements were carried out to identify the crystal structure of the as-prepared PbS crystals. Typically, the XRD patterns of the distinct octahedral, star-shaped, and cubic PbS crystals are shown in Fig. 1. It indicates that all of them possess a face-centered-cubic (FCC) structure and the peaks match well with the literature data (JCPDS card, File No.05–0592). No impurity peaks from Pb metal or PbO are present in these patterns, except the presence of diffraction peaks originating from the ITO substrate. The strong and sharp peaks suggest that the as-synthesized crystals have a high degree of crystallinity. There is little change in the intensity ratio between the (200) and (111) diffraction peaks in spite of the distinct crystal shapes, because the PbS crystals are randomly oriented on the substrate and the diffractometer collects reflections only from the crystallographic planes parallel to the substrate. However, in the case of the cubic PbS crystals, a strong reflection from the (311) facets is observed, indicating the cubes may be dominantly oriented with the (311) facets parallel to the ITO substrate.

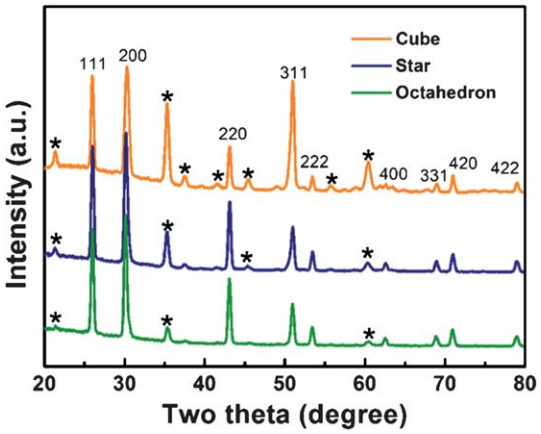

Fig. 1 XRD patterns of PbS crystals with different morphologies, the asterisk represents the peaks from the ITO substrate. The $PbCl_2$ concentrations for the electrodeposition of octahedral, star-shaped, and cubic PbS crystals are 0.027 g, 0.022 g, and 0.010 g, respectively.

In order to discuss the preferential growth and shape evolution of our PbS crystals, we used electron backscatter diffraction pattern (EBSD) to confirm whether or not our as-prepared PbS structures are single crystals and to identify the orientation of the exposed crystal facets. As seen from the EBSD data of a single cubic PbS structure (Fig. 2a), the Kikuchi pattern obtained clearly shows that the electrodeposited PbS crystals are single crystals and the bands in the pattern representing the reflecting facets in the diffracting crystal volume can be precisely indexed to FCC structured PbS crystals (space group: Fm3m (225), JCPDS card, File No.05–0592), which is consistent with the XRD results. From the inverse pole figure (Fig. 2d), it can be found that the detected facet is the (001) facet of the cubic crystal. Considering the detected surface of the crystal is parallel to the ITO substrate (illustrated by Fig. 2c), it is confirmed that the cubic PbS crystals are enclosed with (100) group facets and the octahedral crystals are deduced to be enclosed with (111) group facets.

The complete shape evolution route of the electrodeposited PbS crystals is illustrated in Fig. 3, where the morphologies of the crystals are clearly shown to first change from octahedral shapes, to star-shaped, to football-like, and finally to cubic crystals with the gradual decrease of $PbCl_2$ concentration. The detailed evolution suggests that we recorded almost every key morphological transformation from octahedral to cubic PbS crystals. Such a clear evolutionary picture of semiconductor crystals, to our best knowledge, is unprecedented. Besides, observations from the low magnification SEM images suggest that we can obtain uniform PbS crystals with a defined morphology and size in a large amount (ESI, Fig. S1†).

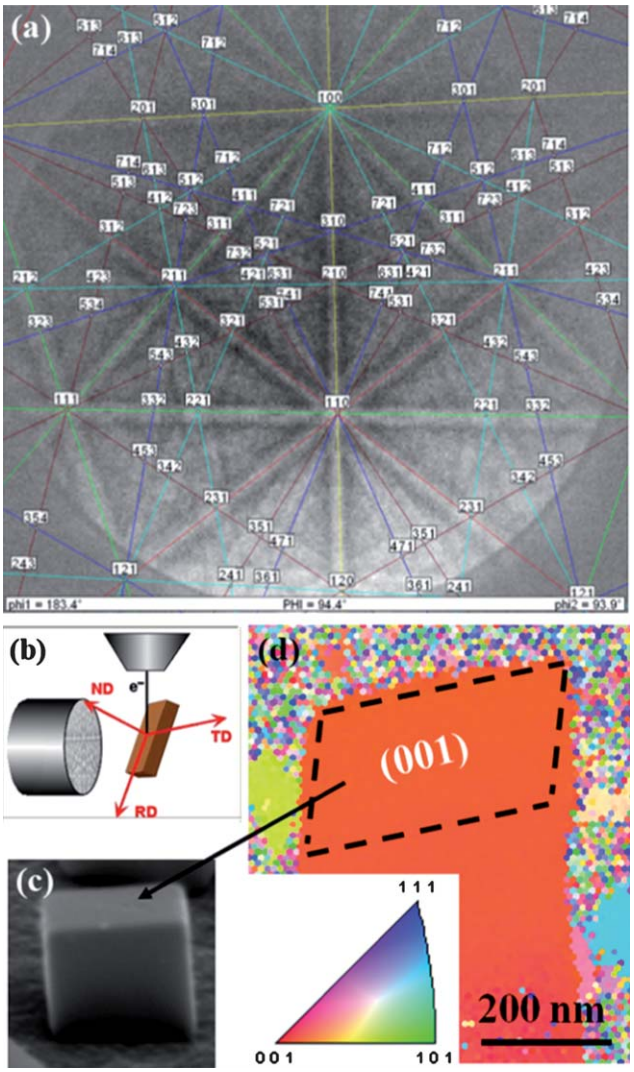

Fig. 2 EBSD patterns of the cubic PbS crystals: (a) indexed Kikuchi Pattern; (b) sample direction of the measurement; (c) a PbS cubic with a surface almost parallel to the substrate; (d) inverse pole <h k l> map in the sample direction of [RD TD ND] = [001] of the PbS cubic in (c). The angular distance between the obtained crystal orientation and the (001) is ~3.5°, consistent with the angular difference between the detected PbS surface and the substrate.

Branching growth and crystal habit growth have been demonstrated to be two main processes that determine the final morphology of crystals for their solution preparation. Branching growth, which is mainly determined by diffusion effect, usually occurs under conditions where the accommodation of growth units is so fast that a depletion zone forms around a growing crystal at the crystal/solution interface and the supersaturation increases with the distance into the parent phase.[12] As a result, the apexes that protrude into the region of higher concentration grow faster than the rest of the facets to form branches. Crystal habit is determined by the relative order of surface energy. Crystals grow faster in the direction perpendicular to the facet with higher surface energy, resulting in shrinking of the higher energy surfaces and increasing of the lower energy surfaces in area.[40,41] Crystal habit, however, can be modified by purposely changing the surface energy of a facet with specific surfactants.[11–13,41]

In the present case, the shape transformation from octahedral to star-shaped mainly resulted from branching growth due to the formation of a Pb^{2+} depletion zone around the fast growing crystals. When the concentration of $PbCl_2$ was high (above 0.027 g), the diffusion of Pb^{2+} to growing sites came up with its consumption and therefore octahedral PbS crystals without any branches were obtained (Fig. 3a). However, if the $PbCl_2$ concentration was reduced to 0.025 g, branching growth at the apexes of the octahedral PbS crystals appeared (Fig. 3b). Because it is much easier to form a depletion zone at relatively lower Pb^{2+} concentration, the degree of branching growth will increase with the decrease in $PbCl_2$ concentration. Consequently, star-shaped PbS crystals were obtained at a $PbCl_2$ concentration of 0.022 g (Fig. 3c). Time-resolved formation of the star-shaped PbS crystals supports this growth behavior (Fig. 4). For a very short deposition time (5 s), octahedral PbS crystals with an average size of 100 nm was formed. With increasing the growth time, the apexes of octahedron were gradually growing out of the main body (15 s). When further increasing the deposition time to 45 s, it could be observed that the apexes extended to form branches. Then, the as-mentioned star-liked shape would finally form after a growth period of 75 s.

While the shape variation from octahedral to star-like shape was the result of branching growth, the appearance of (100) facets of the PbS crystals indicates the change of crystal habit. In the case of PbS, crystal habit prefers to form cubic crystals, which is due to the higher intrinsic surface energy of the (111) facets containing Pb or S only, as compared to that of the (100) facets, which contain both Pb and S.[42] Because no additional surfactant was involved in our electrodeposition, we mainly attribute the present crystal habit conversion to the reduction of the Cl^- ion concentration around the growing crystals. The Cl^- ions could preferentially adsorb onto the (111) facets of PbS because of its stronger interaction with the charged (111) facets than the uncharged (100) facets for PbS. As a result, at relatively higher $PbCl_2$ concentration, (111) facets were well stabilized by Cl^- ions and their surface energies were lower than the (100) facets, which resulted in the exposure of the (111) facets for the final shape of the PbS crystals. However, with a decrease in the $PbCl_2$ concentration, the effect of the Cl^- ions became weak and (100) facets started to appear along with the (111) facets due to the comparable growth rate between [111] and [100] directions. As seen in Fig. 3d–3f, the lower the $PbCl_2$ concentration was, the larger the (100) facets became, though the star-like shape remained. With a further decrease in the concentration of Cl^-, the growth rate along the [111] direction exceeded that along the [100] direction, making the (100) facets became dominant and allowing the gradual formation of cubic PbS crystals (Fig. 3i). The important role of Cl^- ions in the shape transformation of PbS crystals during the electrodeposition process was evidenced by replacing $PbCl_2$ with $Pb(NO_3)$ as the Pb precursor. It was found that only cubic or irregular PbS crystals were obtained and no shape change was observed by changing the $Pb(NO_3)_3$ concentration (ESI, Fig. S2†). Besides, morphological changes of Cu_2O[41] and ZnO[43] crystals due to the capping effect of Cl^- ions, as well as effects of concentration of chloride anions on the microstructure of precipitates from lead nitrate solutions[44] were

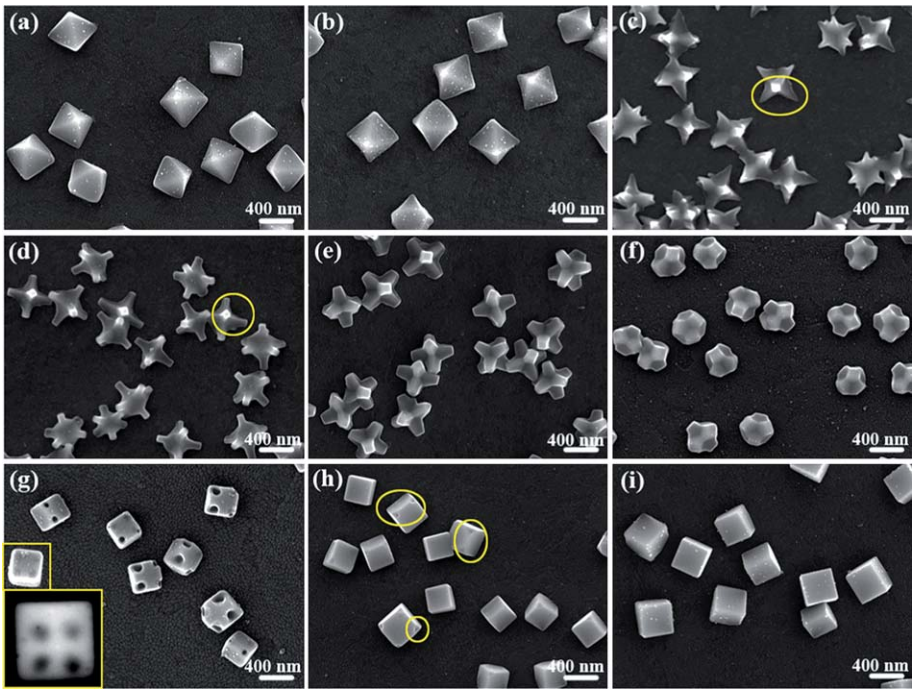

Fig. 3 The shape evolution of PbS crystals with decreasing $PbCl_2$ concentration at a constant deposition current of 0.2 mA and with deposition time of 75 s: (a) 0.027 g, octahedral without branching; (b) 0.025 g, octahedral with appearing branches; (c) 0.022 g, typical star-shaped; (d) 0.020 g, star-shaped with the appearance of (100) facets; (e) 0.018 g, star-shaped with larger (100) facets but shorter branches; (f) 0.016 g, football-like shaped with even larger (100) facets and shorter branches; (g) 0.014 g, partially hollow cubic, with inset showing a typical PbS crystal and its backscattered electron image; (h) 0.012 g, cubic with incompletely formed apexes; (i) 0.010 g, well-defined solid cubic.

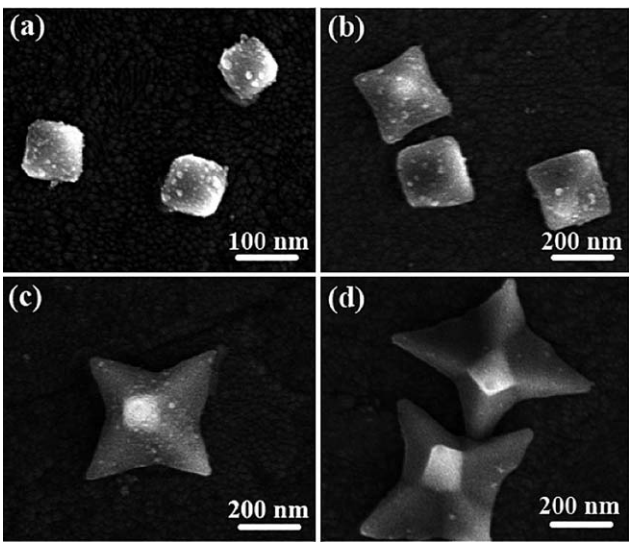

Fig. 4 Time dependent formation of star-shaped PbS crystals with applied current of 0.2 mA and $PbCl_2$ concentration of 0.022 g. SEM images obtained from the sample for different growth time: (a) 5 s; (b) 15 s; (c) 45 s; (d) 75 s.

also previously reported. Furthermore, cubic PbS crystals with a partially hollow structure (Fig. 3g) were recorded for the first time during the evolution, which possibly resulted from the quick encapsulation of PbS crystals by the fast expanding (100) facets.

It is worth mentioning that the Cl^- ion concentration around the growing crystals is not only affected by the initial $PbCl_2$ concentration in the solution, but also by the applied deposition current and deposition time. Under an electric field, cations like Pb^{2+} ions move toward the cathode, while anions like Cl^- ions go to the anode during the electrodeposition, which generates concentration gradients of the ions (Scheme 1). The distribution of the ions is affected by the strength of the applied deposition current (or potential), and could lead to different morphologies of PbS by changing the deposition current even if using the same

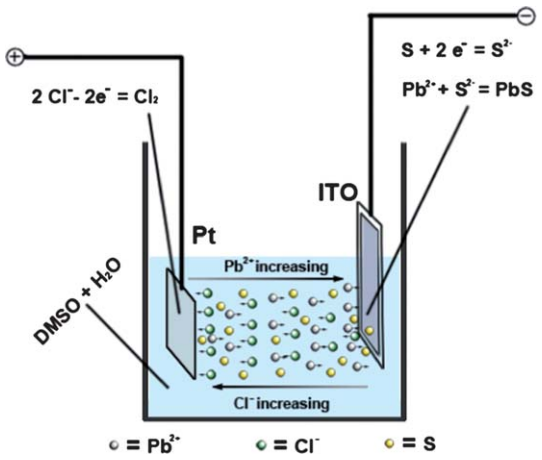

Scheme 1 Illustration of the electrodeposition processes for PbS crystal synthesis. Due to the presence of electrical field, the concentration of Pb^{2+} increases, while the concentration of Cl^- decreases from anode (Pt) to cathode (ITO).

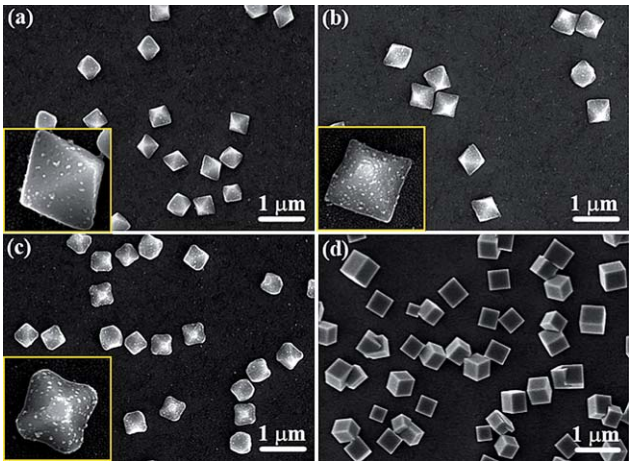

Fig. 5 SEM images of PbS crystals electrodeposited at different currents and $PbCl_2$ concentrations with fixed deposition time of 75 s. (a) 0.05 mA, $PbCl_2$ 0.018 g, with inset showing a well-defined octahedral crystal; (b) 0.05 mA, $PbCl_2$ 0.014 g, with inset showing a branched octahedral crystal; (c) 0.05 mA, $PbCl_2$ 0.010 g, with inset showing a truncated octahedral crystal; (d) 0.4 mA, $PbCl_2$ 0.020 g.

initial precursor concentrations. For instance, when a much lower current density (0.05 mA) was used for PbS electrodeposition with the $PbCl_2$ concentration varying from 0.018 g to 0.010 g, the above shape evolution didn't occur and only octahedral, branched octahedral, and truncated octahedral PbS crystals were observed (Fig. 5a–5c). However, at a larger deposition current density (0.4 mA), cubic PbS crystals formed even though the $PbCl_2$ concentration was as high as 0.022 g (Fig. 5d). These results suggest both initial $PbCl_2$ concentration and applied deposition current have influence on the PbS crystal shape. It seems that they may collaborate with each other to determine the distribution of the ions and in turn their concentration gradient. Furthermore, the concentration of Cl^- ions will change with the deposition time, due to its gradual consumption at the anode by oxidation. For example, as we extended the deposition time to 200 s, the (100) facets appeared (ESI, Fig. S3†) even though we kept the other deposition conditions identical with those for formation of the star-shaped PbS crystals (Fig. 3c). All these observations demonstrate the versatility of the present electrodeposition method for tailoring the morphologies of PbS crystals. We illustrate the morphology variation of PbS crystals along with the change of $PbCl_2$ concentration in Scheme 2. The morphology evolution is the consequence of competition between branching growth and the capping effect of Cl^- ions on the (111) facets of PbS. As demonstrated here, we believe that the systematic tailoring of the morphology of PbS crystals can be easily realized by control over precursor concentrations, deposition current (potential), deposition time, and other relevant parameters of electrodeposition.

Conclusion

In summary, we have demonstrated a new, facile, surfactant-free, one-step electrochemical method for synthesis of PbS crystals with the capability to systematically tune its morphologies. An interesting and successive shape evolution with rich shapes from octahedral to cubic was achieved by elucidating the role of Cl^- ions in this green synthesis route. The detailed transformation provides a powerful framework by which interesting morphologies can be designed and fabricated and by which key properties of growth dynamics can be further investigated. The present electrodeposition method may provide a way for shape-controlled synthesis of other semiconductor crystals, especially for metal sulfides, towards realization of their tunable optoelectronic properties.

Acknowledgements

The authors wish to thank the National Natural Science Foundation of China (grants 50990063, 50973095, 51011130028, and 51002136) for financial support. The work was also partly supported by the Major State Basic Research Development Program of MOST (2007CB613400).

References

1 H. T. Shi, L. M. Qi, J. M. Ma and H. M. Cheng, *J. Am. Chem. Soc.*, 2003, **125**, 3450.
2 S. Mann, *Angew. Chem., Int. Ed.*, 2000, **39**, 3392.
3 X. Lan, J. Y. Zhang, H. Gao and T. M. Wang, *CrystEngComm*, 2011, **13**, 633.
4 N. N. Zhao and L. M. Qi, *Adv. Mater.*, 2006, **18**, 359.
5 S. M. Lee, S. N. Cho and J. Cheon, *Adv. Mater.*, 2003, **15**, 441.
6 F. L. Jia, K. W. Wong and L. Z. Zhang, *J. Phys. Chem. C*, 2009, **113**, 7200.
7 M. Z. Zhang, G. H. Zuo, Z. C. Zong, H. Y. Cheng, Z. He, C. M. Yang and G. T. Zou, *Small*, 2006, **2**, 727.
8 L. F. Xu, Q. W. Chen and D. S. Xu, *J. Phys. Chem. C*, 2007, **111**, 11560.

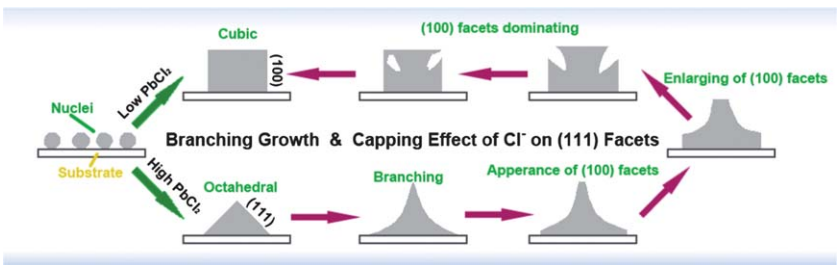

Scheme 2 Illustration of the shape evolution process of PbS crystals at deposition current of 0.2 mA for 75 s deposition time. At high $PbCl_2$ concentration octahedral PbS crystals form, while cubic PbS crystals are obtained at low $PbCl_2$ concentration (the green arrows). With the decrease of $PbCl_2$ concentration (the red arrows), a successive evolution can be observed.

9 G. W. She, X. H. Zhang, W. S. Shi, X. Fan, J. C. Chang, C. S. Lee, S. T. Lee and C. H. Liu, *Appl. Phys. Lett.*, 2008, **92**, 053111.
10 Z. Y. Yin, S. X. Wu, X. Z. Zhou, X. Huang, Q. C. Zhang, F. Boey and H. Zhang, *Small*, 2010, **6**, 307.
11 H. S. Jang, S. J. Kim and K. S. Choi, *Small*, 2010, **6**, 2183.
12 M. J. Siegfried and K. S. Choi, *Angew. Chem., Int. Ed.*, 2008, **47**, 368.
13 C. M. McShane and K. S. Choi, *J. Am. Chem. Soc.*, 2009, **131**, 2561.
14 G. R. Li, F. L. Zheng and Y. X. Tong, *Cryst. Growth Des.*, 2008, **8**, 1226.
15 G. W. She, X. H. Zhang, W. S. Shi, Y. Cai, N. Wang, P. Liu and D. M. Chen, *Cryst. Growth Des.*, 2008, **8**, 1789.
16 Y. X. Nan, F. Chen, L. G. Yang and H. Z. Chen, *J. Phys. Chem. C*, 2010, **114**, 11911.
17 J. L. Machol, F. W. Wise, R. C. Patel and D. B. Tanner, *Phys. Rev. B: Condens. Matter*, 1993, **48**, 2819.
18 M. Fardy, A. I. Hochbaum, J. Goldberger, M. J. M. Zhang and P. D. Yang, *Adv. Mater.*, 2007, **19**, 3047.
19 D. M. N. M. Dissanayake, A. A. D. T. Adikaari and S. R. P. Silva, *Appl. Phys. Lett.*, 2008, **92**, 093308.
20 S. A. McDonald, G. Konstantatos, S. Zhang, P. W. Cyr, E. J. D. Klem, L. Levina and E. H. Sargent, *Nat. Mater.*, 2005, **4**, 138.
21 C. Ratanatawanate, Y. Tao and K. J. Balkus, Jr, *J. Phys. Chem. C*, 2009, **113**, 10755.
22 J. Akhtar, M. A. Malik, P. O'Brien, K. G. U. Wijayantha, R. Dharmadasa, S. J. O. Hardman, D. M. Graham, B. F. Spencer, S. K. Stubbs, W. R. Flavell, D. J. Binks, F. Sirotti, M. E. Kazzi and M. Silly, *J. Mater. Chem.*, 2010, **20**, 2336.
23 H. B. Li, D. Chen, L. L. Li, F. Q. Tang, L. Zhang and J. Ren, *CrystEngComm*, 2010, **12**, 1127.
24 J. H. Warner and H. Q. Cao, *Nanotechnology*, 2008, **19**, 305605.
25 M. J. Bierman, Y. K. A. Lau and S. Jin, *Nano Lett.*, 2007, **7**, 2907.
26 Y. K. A. Lau, D. J. Chernak, M. J. Bierman and S. Jin, *J. Am. Chem. Soc.*, 2009, **131**, 16461.
27 S. Y. Jang, Y. M. Song, H. S. Kim, Y. J. Cho, Y. S. Seo, G. B. Jung, C. W. Lee, J. H. Park, M. K. Jung, J. H. Kim, B. S. Kim, J. G. Kim and Y. J. Kim, *ACS Nano*, 2010, **4**, 2391.
28 J. M. Luther, H. M. Zheng, B. Sadtler and A. P. Alivisatos, *J. Am. Chem. Soc.*, 2009, **131**, 16851.
29 Y. N. Wang, Q. Q. Dai, X. Y. Yang, B. Zou, D. M. Li, B. B. Liu, M. Z. Hu and G. T. Zou, *CrystEngComm*, 2011, **13**, 199.
30 F. Zuo, S. Yan, B. Zhang, Y. Zhao and Y. Xie, *J. Phys. Chem. C*, 2008, **112**, 2831.
31 B. Ding, M. M. Shi, F. Chen, R. J. Zhou, M. Deng, M. Wang and H. Z. Chen, *J. Cryst. Growth*, 2009, **311**, 1533.
32 S. Z. Liu, S. L. Xiong, K. Y. Bao, J. Cao and Y. T. Qian, *J. Phys. Chem. C*, 2009, **113**, 13002.
33 N. Wang, X. Cao, L. Guo, S. H. Yang and Z. Y. Wu, *ACS Nano*, 2008, **2**, 184.
34 H. Saloniemi, M. Kemell, M. Ritala and M. Leskela, *Thin Solid Films*, 2001, **386**, 32.
35 K. K. Nanda and S. N. Sahu, *Adv. Mater.*, 2001, **13**, 280.
36 F. Chen, W. M. Qiu, X. Q. Chen, M. Wang and H. Z. Chen, *CrystEngComm*, 2010, **12**, 1893.
37 W. X. Niu, L. Zhang and G. B. Xu, *ACS Nano*, 2010, **4**, 1987.
38 S. M. Lee, Y. W. Jun, S. N. Cho and J. W. Cheon, *J. Am. Chem. Soc.*, 2002, **124**, 11245.
39 A. Radi, D. Pradhan, Y. K. Sohn and K. T. Leung, *ACS Nano*, 2010, **4**, 1553.
40 T. K. Sau and A. L. Rogach, *Adv. Mater.*, 2010, **22**, 1781.
41 K. S. Choi, *Dalton Trans.*, 2008, **40**, 5432.
42 Y. W. Jun, J. H. Lee, J. S. Choi and J. W. Cheon, *J. Phys. Chem. B*, 2005, **109**, 14795.
43 L. F. Xu, Y. Guo, Q. Liao, J. P. Zhang and D. S. Xu, *J. Phys. Chem. B*, 2005, **109**, 13519.
44 J. Cheng, X. P. Zou, W. L. Song, X. M. Meng, Y. Su, G. Q. Yang, X. M. Lü, F. X. Zhang and M. S. Cao, *CrystEngComm*, 2010, **12**, 1790.

